Journal of Microscopy and Ultrastructure 5 (2017) 9–20

Contents lists available at ScienceDirect

Journal of Microscopy and Ultrastructure

journal homepage: www.elsevier.com/locate/jmau

Original Article

Ultrastructure of the salivary glands, alimentary canal and bacteria-like organisms in the Asian citrus psyllid, vector of citrus huanglongbing disease bacteria

El-Desouky Ammar[a,b,*], David G. Hall[a], Robert G. Shatters Jr[a]

[a] USDA-ARS, US Horticultural Research Laboratory, Fort Pierce, FL 34945, USA
[b] University of Florida, IFAS, Fort Pierce, FL 34945, USA

ARTICLE INFO

Article history:
Received 10 November 2015
Received in revised form 20 January 2016
Accepted 26 January 2016
Available online 1 February 2016

Keywords:
alimentary canal
bacteriome
bacterium-like structures
salivary gland
symbionts

ABSTRACT

The Asian citrus psyllid (ACP, *Diaphorina citri*, Hemiptera: Liviidae) is the principal vector of *Candidatus* Liberibacter asiaticus (Las), the putative bacterial agent of citrus greening/huanglongbing (HLB); currently the most serious citrus disease worldwide. Las is transmitted in a persistent–propagative manner by ACP, and the salivary glands and midgut have been suggested as transmission barriers that can impede translocation of Las within the vector. However, no detailed ultrastructural studies have been reported on these organs in this or other psyllid species, although some bacterium-like structures have been described in them and assumed to be the causal agents of HLB. In this study, we describe the ultrastructure of the salivary glands, filter chamber, other parts of the alimentary canal, and other organs and tissues of ACP including the compound ganglionic mass (in the thorax) and the bacteriome (in the abdomen). Furthermore, in addition to two ultrastructurally apparently different symbiotic bacteria found in the bacteriome, other morphological types of bacteria were found in the gut epithelial cells and salivary glands of both Las-infected (quantitative polymerase chain reaction positive) and noninfected (quantitative polymerase chain reaction negative) ACP. These results show the importance of immunolabeling, fluorescence *in situ* hybridization, or other labeling techniques that must be used before identifying any bacterium-like structures in ACP or other vectors as Las or other possible agents of HLB. This ultrastructural investigation should help future work on the cellular and subcellular aspects of pathogen–psyllid relationships, including the study of receptors, binding sites, and transmission barriers of Las and other pathogens within their psyllid vectors.

1. Introduction

Psyllids (jumping lice, Hemiptera: Psylloidea) comprise a group of around 3000 species of small plant-sap sucking insects that occur throughout nearly all the world's major climatic regions where suitable host plants are found [1]. Several psyllid species have been reported as vectors of plant viral and bacterial pathogens causing some of the most serious diseases of several economically important crops [1]. The Asian citrus psyllid (ACP), *Diaphorina citri* Kuwayama (Liviidae), is the principal vector of *Candidatus* Liberibacter asiaticus (Las) and *C.* Liberibacter americanus; two of the putative causal bacteria of huanglongbing (HLB, or citrus greening), which is currently the most devastating citrus disease worldwide [2–4]. HLB-associated bacteria are transmitted in a persistent–propagative manner by

* Corresponding Author:
E-mail address: desoukyammar@gmail.com (E.-D. Ammar).

http://dx.doi.org/10.1016/j.jmau.2016.01.005
2213-879X/

ACP in the USA, Asia, and South and Central America, and by another psyllid, *Trioza erytreae* (Del Guercio) (Triozidae) in African countries [2,4–7]. Additionally, the potato psyllid *Bactericera cockerelli* (Hemiptera: Triozidae) has been found more recently to vector *Candidatus* Liberibacter solanacearum (Lso), the putative causal agent of zebra chip and other diseases of potatoes, tomatoes and other crops [8,9]. Using fluorescence *in situ* hybridization and/or quantitative polymerase chain reaction (qPCR) methods, both Las and Lso were reported to infect most of the vector psyllid organs, including the salivary glands and alimentary canal; both of which are suggested transmission barriers that can impede the translocation of Las and Lso bacteria within their vectors [9–12]. However, no detailed ultrastructural studies have been done on these important organs in these or other psyllid species, although some early investigations reported bacterium-like structures that were assumed to be the causal agents of HLB in *D. citri* [13,14] and T. *erytreae* [15]. Understanding the cellular and subcellular structures is important in studying pathogen–vector relations, especially when looking at transmission barriers, binding sites and receptors for viral and bacterial pathogens in their insect vectors [16,17].

In the present work, as part of a wider study on ACP–Las vector relations, we examined the ultrastructure of the salivary glands, alimentary canal and other organs in nymphs and adults of ACP. We also report bacterium-like structures in the bacteriome, alimentary canal and salivary glands of both Las-infected (qPCR positive) and noninfected (qPCR negative) ACP. It is hoped that this study will help future work on the cellular and subcellular aspects of pathogen–psyllid relationships, including the question of transmission barriers of Las, Lso and other pathogens within their psyllid vectors.

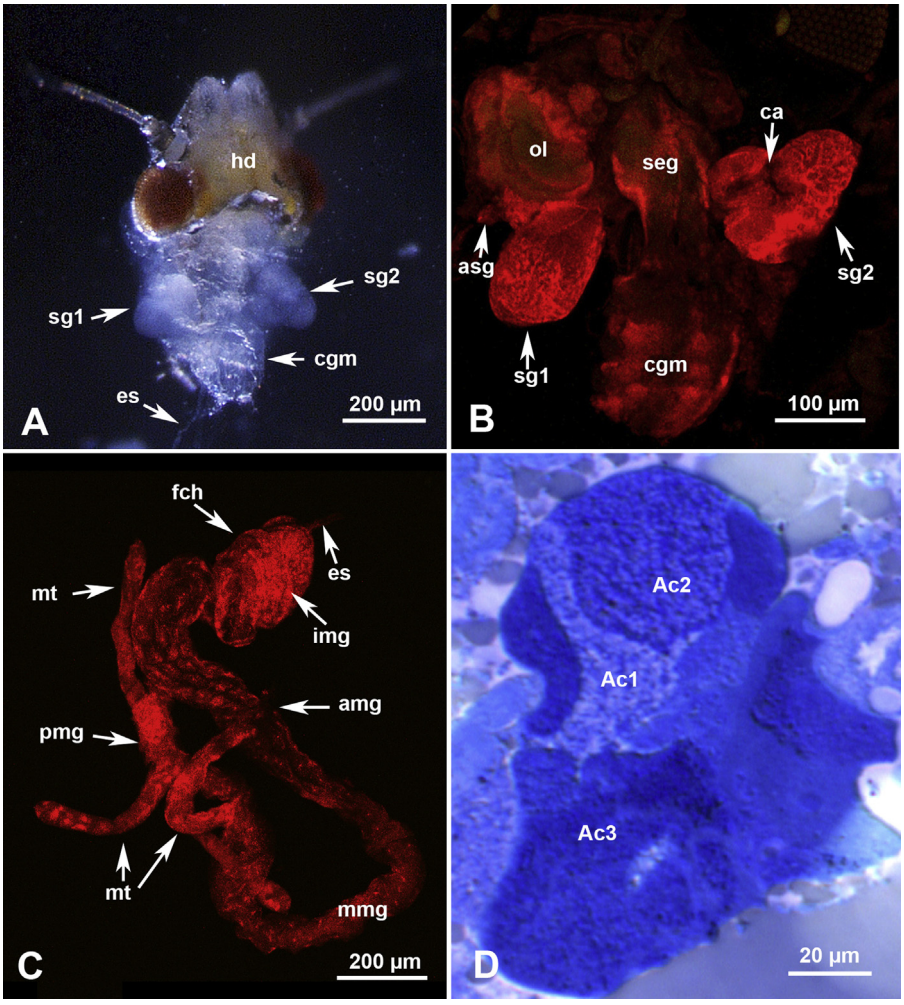

Fig. 1. Gross morphology of the salivary glands, alimentary canal and compound ganglionic mass in *Diaphorina citri*. (A) Stereomicrograph of partially dissected head (hd) and thorax showing two salivary glands (sg1 and sg2), compound ganglionic mass (cgm) and esophagus (es). (B) Confocal micrograph of the two principal salivary glands (sg1 and sg2), an accessory salivary gland (asg), compound ganglionic mass (cgm), sub-esophageal ganglion (seg), and optic lope (ol); note the intercellular canaliculi (ca) between various acini/secretory cells. (C) Confocal micrograph of a dissected alimentary canal showing the esophagus (es), filter chamber (fch), anterior midgut (amg), middle midgut (mmg), posterior midgut (pmg), and Malpighian tubules (mt); within the filter chamber the inner posterior midgut (img) is coiled with several loops inside the anterior-most part of the midgut. (D) Semithin section (stained with toluidine blue) in the principal salivary gland showing at least three differentially stained acini/groups of secretory cells (Ac1, Ac2 and Ac3).

2. Materials and methods

Healthy (non-Las exposed) adult ACP were from our laboratory colony that has been maintained on young healthy citrus (*Citrus macrophylla* Wester) or orange jasmine (*Murraya exotica* L.) plants in the greenhouse. Las-exposed insects were collected from HLB-infected citrus trees (showing HLB symptoms) in Picos Farm, ARS-USDA, Fort Pierce, FL, USA. To make sure that each insect from the Las-exposed or nonexposed groups was either Las-positive or Las-negative, before processing it for thin sectioning transmission electron microscopy (TEM), each adult was dissected in phosphate-buffered saline under a stereomicroscope (at 20×) into three parts: (1) midgut and filter chamber; (2) head and thorax (including salivary glands); and (3) abdomen (without most of the gut). The second or third part from each insect was stored in the freezer and later tested for Las by qPCR with Li primers [18]. Insect parts that were not frozen for qPCR were immersed immediately following dissection into the prefixative (3% glutaraldehyde in phosphate buffer, pH 7.4). These specimens were fixed overnight at 4 °C, postfixed in 1% osmium tetroxide in the same buffer for 1 hour, washed in buffer, dehydrated in ethanol and propylene oxide, and embedded in Spurr's resin [19].

Semi-thin sections (1–2 μm thick) stained with toluidine blue were observed by light microscopy to select certain ACP parts or organs for thin sectioning. Ultrathin sections (~80 nm thick), cut with an ultramicrotome (Leica EM UC7), were mounted on 200–300 mesh noncoated copper grids. These sections were stained with uranyl acetate and lead citrate and examined at 25 kV

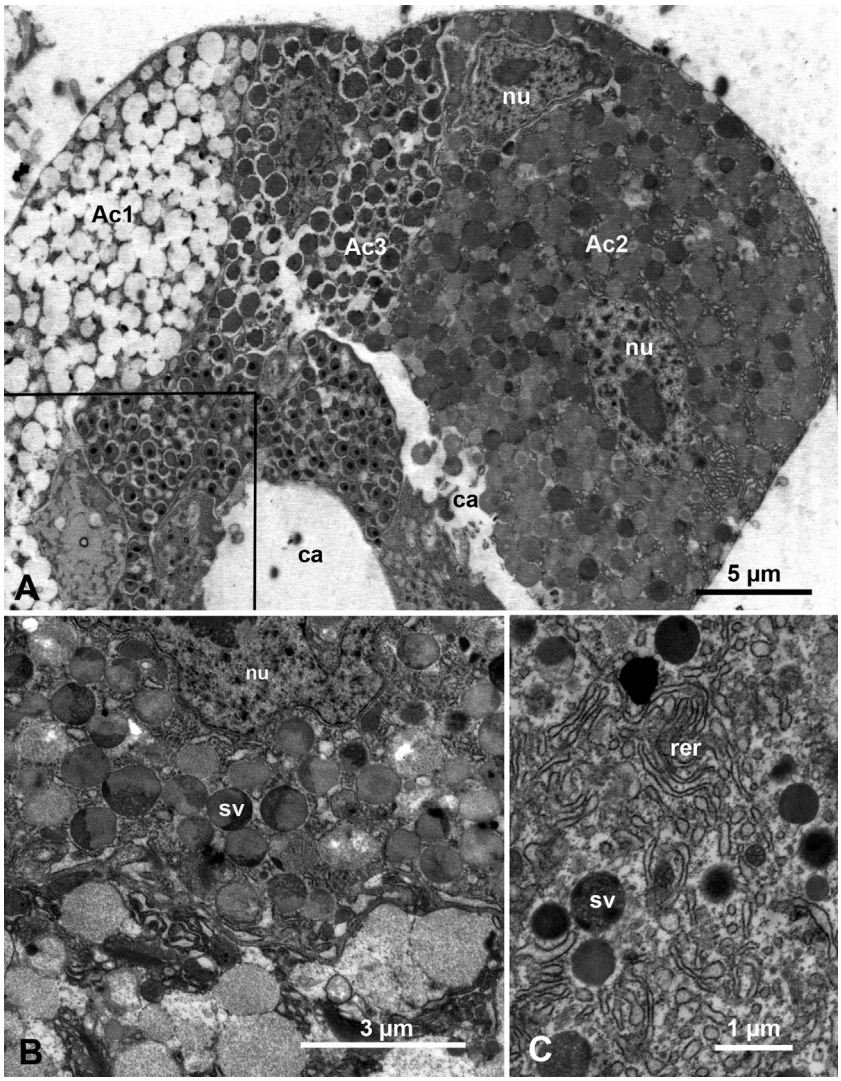

Fig. 2. Ultrastructure of the principal salivary gland in *Diaphorina citri* (A) nymphs and (B, C) adults. (A) Part of the principal salivary gland showing three types of acini: Ac1 with electrolucent secretory vesicles, Ac2, with both semiopaque and electron-dense secretory vesicles, and Ac3 with mainly electron-dense secretory vesicles; boxed area is shown at higher magnification in Figure 4A; note the intercellular canaliculi (ca) between acini and the two nuclei (nu) in acinus Ac2. (B) Part of acinus Ac2 showing the nu and secretory vesicles (sv) with various electron-dense or semiopaque material. (C) Electron-dense sv and surrounding cytoplasm, rich with rough endoplasmic reticulum (rer).

using a scanning transmission electron microscope (S-4800; Hitachi, Pleasanton, CA, USA) in the TEM mode at magnifications up to 20,000×.

Twenty Las-exposed and six Las-unexposed adults were processed by qPCR. Eight of the Las-exposed adults proved qPCR-positive for Las, and six of these (with CT values of 27.4–32.5) were processed and sectioned for TEM. Four control (non-Las exposed, qPCR negative) adults were similarly processed. Also, some non-Las exposed nymphs of ACP from our healthy colony were similarly processed, sectioned, and examined. Several grids (with multiple sections on each) from the head, thorax, abdomen, and dissected alimentary canal of various insects from the Las-infected or noninfected ACP were examined by TEM.

Additionally, for studying the gross morphology of ACP alimentary canal and salivary glands, these organs were dissected, fixed in 4% paraformaldehyde, and stained with the nuclear stain propidium iodide, then examined by confocal laser scanning microscopy, as described previously [10]. Furthermore, the bacteriome in whole ACP nymphs (1^{st}–3^{rd} instars), which were fixed in 4% paraformaldehyde, was examined with epifluorescence microscopy with UV light, as described previously [20].

3. Results and discussion

3.1. Location and gross morphology of various ACP organs

In ACP, the principal salivary glands were two heart-shaped, white colored, semiopaque organs located in the thorax, mainly in the first and second thoracic segments, dorsal to the whitish more opaque compound ganglionic mass (CGM; Figures 1A and 1B). The two accessory salivary glands are smaller tubular structures attached to the principal salivary glands anterolaterally (Figure 1B, asg). The CGM, in the pear psyllid *Psylla mali*, has been termed the thoracic ganglion by Brittain [21], but it is more likely an amalgamation of the thoracic and abdominal ganglia as reported for several other hemipterans [22,23]. In

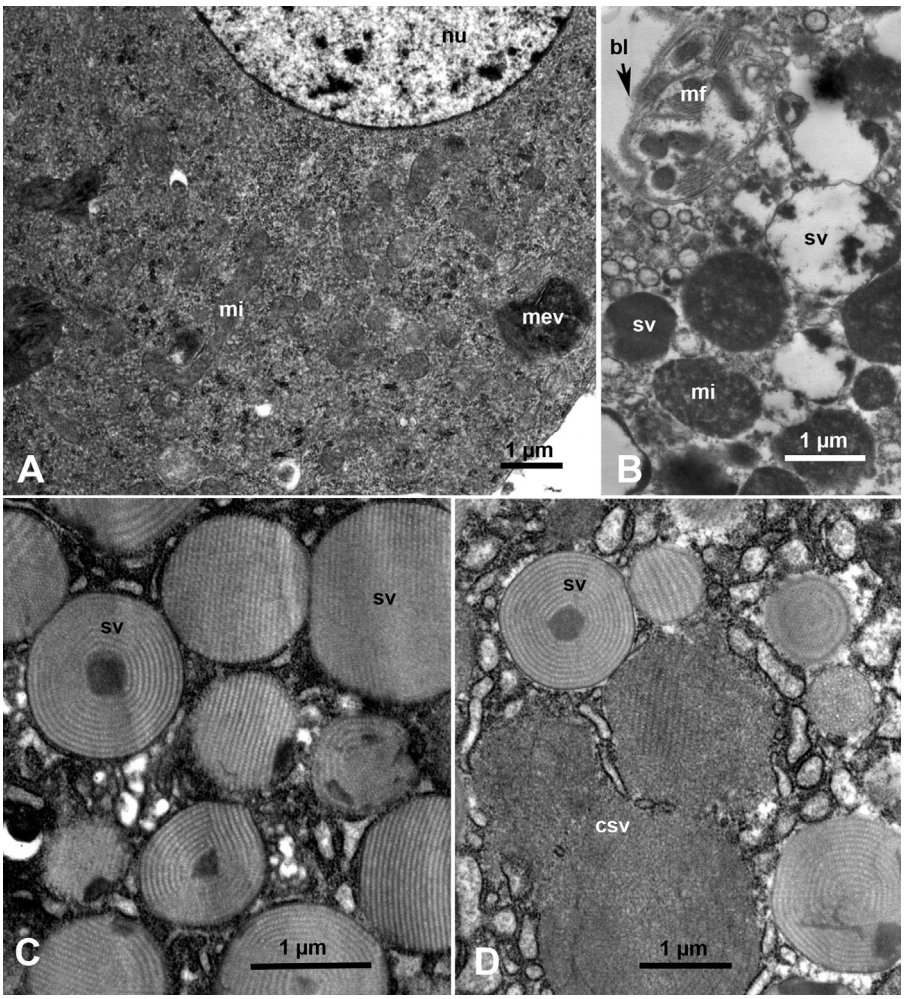

Fig. 3. Ultrastructure of the principal and accessory salivary glands in *Diaphorina citri* adults. (A) An accessory salivary gland cell with abundant mitochondria (mi), membranous vesicles, (mev) and large nucleus (nu). (B) Muscle fibers (mf) under the basal lamina (bl) at the periphery of a principal salivary gland cell, with mi, and secretory vesicles (sv); some with partially emptied darkly stained material. (C, D) sv in the principal salivary gland cells, containing crystalline material in various forms, with three of these vesicles apparently coalescing with one another (csv).

ACP, the esophagus, which connects the cibarium (sucking pump) and the midgut, is a narrow tube that runs posteriorly between the two salivary glands dorsal to the subesophageal ganglion and the CGM, before entering the filter chamber part of the alimentary canal (Figures 1A and 1C, es). The inner posterior midgut, which is looped inside the outer-anterior midgut in the filter chamber region [24], can be seen in the confocal image shown in Figure 1C, img. Posterior to the filter chamber, the wider part of the midgut (anterior or descending midgut) leads to a narrower part (middle midgut) followed by another narrow part (posterior or ascending midgut); the terminal part of which enters the filter chamber and loops inside it as mentioned above. The posterior/ascending midgut is joined by four separate Malpighian tubules (Figure 1C, mt) before entering the filter chamber. Most of the alimentary canal parts, starting with the filter chamber, are found in the abdomen, along with the reproductive system, fat tissue, and bacteriome. Ultrastructure of the oral region in the potato psyllid *B. cockerelli* has been studied in detail by Cicero et al. [25], and the reproductive system in two other psyllid spp. has been described earlier [26,27] and thus will not be described or discussed here.

3.2. Salivary glands

Ultrastructure of the principal salivary glands in ACP nymphs and adults is shown in Figures 2A and 2B. The principal salivary gland secretory cells (acini) are large with large double nuclei and abundant rough endoplasmic reticulum and secretory vesicles of various electron densities. At least three types of acini can be distinguished: Ac1 with electron lucent secretory vesicles;

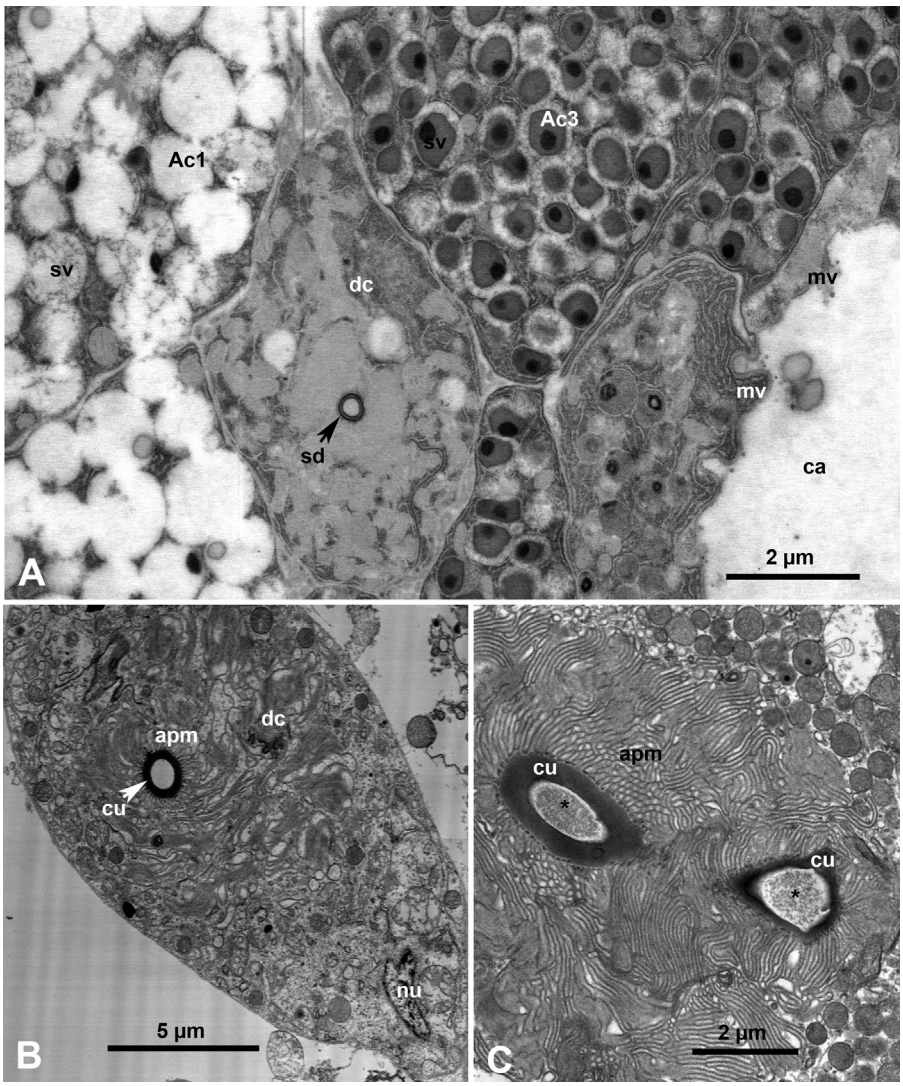

Fig. 4. Ultrastructure of the salivary glands and salivary ducts in *Diaphorina citri*. (A) Higher magnification of the boxed area in Figure 2A, showing two types of acini (Ac1 and Ac3), salivary duct cells (dc), salivary duct (sd), and a large intercellular canaliculum (ca) lined with microvilli (mv). (B, C) Cross-sections in the salivary ducts, the lumen of which is lined with a cuticle (cu), surrounded by elaborate infoldings of the apical plasma membrane (apm) of dc; asterisks indicate semiopaque material (putative salivary secretions) in the duct lumen; nu, nucleus.

Ac2, with both semiopaque and electron-dense secretory vesicles; and Ac3 with mainly electron-dense secretory vesicle (Figures 1D and 2A–2C). In cells of the smaller accessory salivary gland, only darkly stained membranous vesicles (that could be also interpreted as darkly stained mitochondria), in addition to abundant elongated (narrower and less dark) mitochondria were found (Figure 3A, mi). The abundance of mitochondria and the observation that many mitochondria appear to be enlarged/elongated, as well as the paucity of secretory vesicles in the accessory salivary gland, suggests that this gland may have a primary function in energy production. Perhaps these accessory salivary glands produce ATP to support the energy-intensive secretory processes carried out by the primary salivary gland cells.

In the principal salivary glands, some of the secretory vesicles containing darkly stained contents appeared to be partially empty (Figure 3B, sv). Other secretory vesicles of the principal salivary glands contained crystalline material in various forms (concentric or linear; Figures 3C and 3D , sv), and some of these vesicles appeared to coalesce with one another (Figures 3C and 3D, csv). It is possible that this crystalline structure is a transitory phase in the secretion process since inside the coalescing vesicles some parts of their secretions appear crystalline while some other parts are probably not (Figure 3D, csv). Up to 13 types

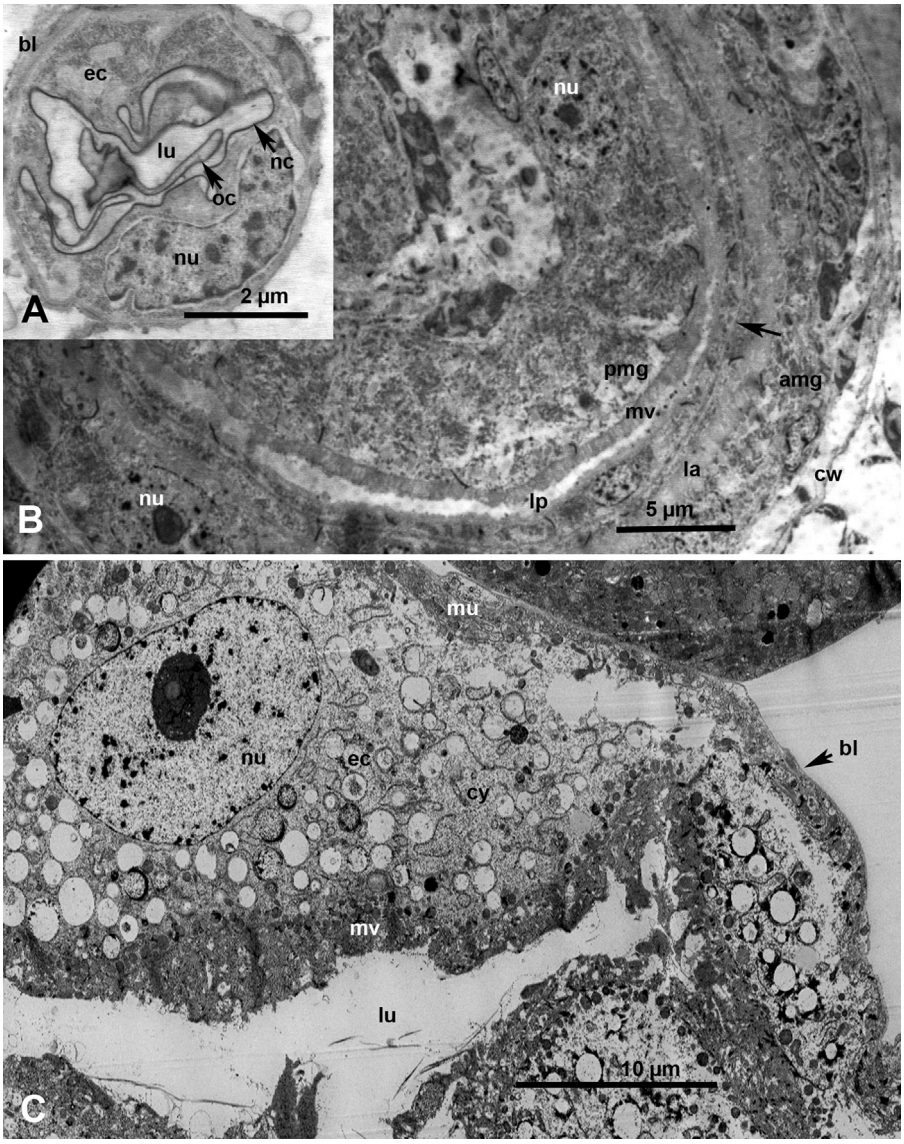

Fig. 5. Ultrastructure of the esophagus, filter chamber and anterior midgut of *Diaphorina citri* (A, B) nymphs and (C) adults. (A) Esophagus of a premolting nymph, showing basal lamina (bl), epithelial cell (ec) with nucleus (nu), lumen (lu), and new (nc), and old (oc) cuticular lining. (B) Cross-section in part of the filter chamber, showing chamber wall (cw), followed by flat cells of the anterior midgut (amg) and (coiled inside) posterior midgut (pmg); note the closely apposed basal lamina of both anterior and posterior midgut (unlabeled arrow). (C) Cross-section of the free part of the anterior midgut (outside the filter chamber) showing large ec with vacuolated cytoplasm (cy), lined with extensive microvilli (mv), with an outer muscular layer (mu) and bl.
la, lumen of anterior midgut; lp, lumen of posterior midgut.

of acini with differently stained secretory vesicles have been described in the salivary glands of other hemipterans, including leafhoppers [28], planthoppers [19,29], whiteflies [30] and Reduviid bugs [31]. However, it is not known whether these types of secretory vesicles remain consistently the same, that is, characteristic for each type, as reported in planthoppers [29], or if they are developmental stages/phases that can transform into one another under various feeding and/or physiological conditions as suggested for some other insects [32].

In ACP, muscle fibers were detected under the basal lamina surrounding cells of the principal salivary gland (Figure 3B, mf), which has been reported earlier with some other hemipterans, including leafhoppers, planthoppers, and Reduviid bugs [19,31], whereas in aphids, a single myoepithelioid cell was reported in the principal salivary gland [33]. In the planthopper *Peregrinus maidis*, muscle fibers, occasionally supplied with small tracheoles, were frequently innervated by small axons surrounded by glial cells [19]. It has been suggested that, at least in these

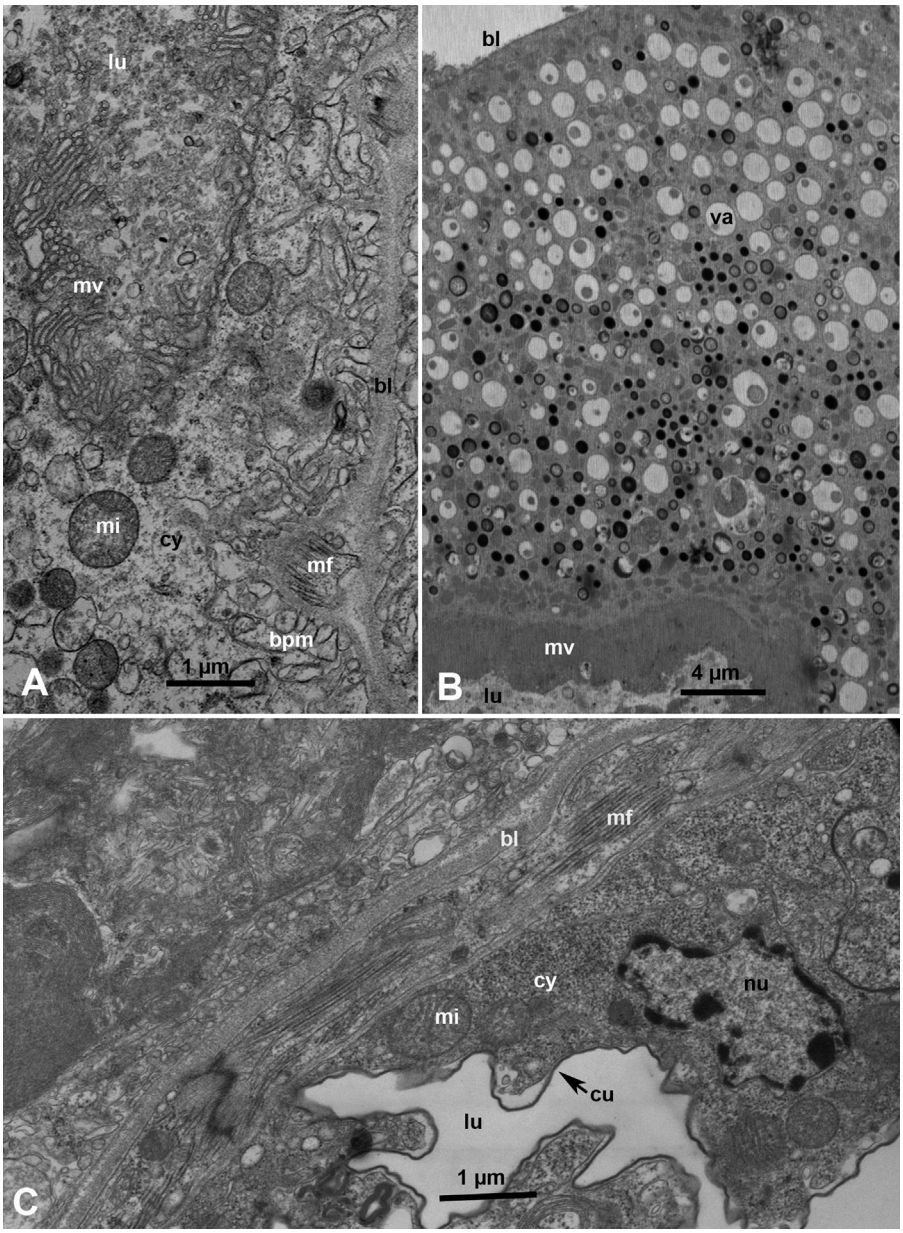

Fig. 6. Ultrastructure of the midgut, Malpighian tubule and hindgut in *Diaphorina citri* adults. (A) Higher magnification of part of an epithelial cell of the midgut, showing basal lamia (bl), muscle fibers (mf), invaginated basal plasma membrane (bpm), cytoplasm (cy), mitochondria (mi), microvilli (mv), and lumen (lu). (B) Part of an epithelial cell of a Malpighian tubule, lined with fine mv, with various-sized cytoplasmic vacuoles (va) either apparently empty, partially full or full of dark excretory material; bl, basal lamina. lu, lumen. (C) Part of the epithelium of the hind gut showing circular mf, bl, nucleus (nu), mi, cy, and cuticular lining (cu) around the lu.

hemipterans, besides pinocytosis, muscle fibers/myofibrils may provide an additional mechanism for transporting secretory/salivary material from secretory vesicles into the intercellular canaliculi and salivary ductules (inside the salivary gland), and from these to the salivary duct connected to each gland [19]. Intercellular canaliculi, with large lumina, lined with microvilli, in ACP principal salivary gland can be seen in the confocal image shown in Figure 1B, ca and in the electron micrographs in Figures 2A and 4A, ca. In ACP, as in other hemipteran insects studied, the lumen of the salivary ducts is lined with cuticle surrounded by extensive and elaborate infoldings of the apical plasma membrane of duct cells (Figures 4A–4C) that produce this cuticle. Semiopaque material, interpreted as putative salivary secretions, was observed in the lumen of some ACP salivary ducts (Figure 4C, asterisks). Salivary secretions probably move from the salivary ducts to the salivary canal in the maxillary stylets, using a special organ: the salivary pump or syringe, previously reported in leafhoppers, aphids and psyllids [22,24,33,34]. This pump/syringe usually has a cuticular piston-like structure, an afferent duct connected to the common salivary duct, and an ejaculatory (or efferent) duct that injects saliva into the salivary canal inside the maxillary stylets [22].

Hemipteran insects are known to produce two types of saliva: soluble (watery) saliva and nonsoluble (gelling) saliva, with mostly the latter forming the salivary or stylet sheaths in/on host plant tissues during probing, feeding, and stylet penetration [35], but it is not yet known which types of acini produce each type of saliva. Most chemical studies on hemipteran salivary components have been done on aphid saliva in which several proteins have been

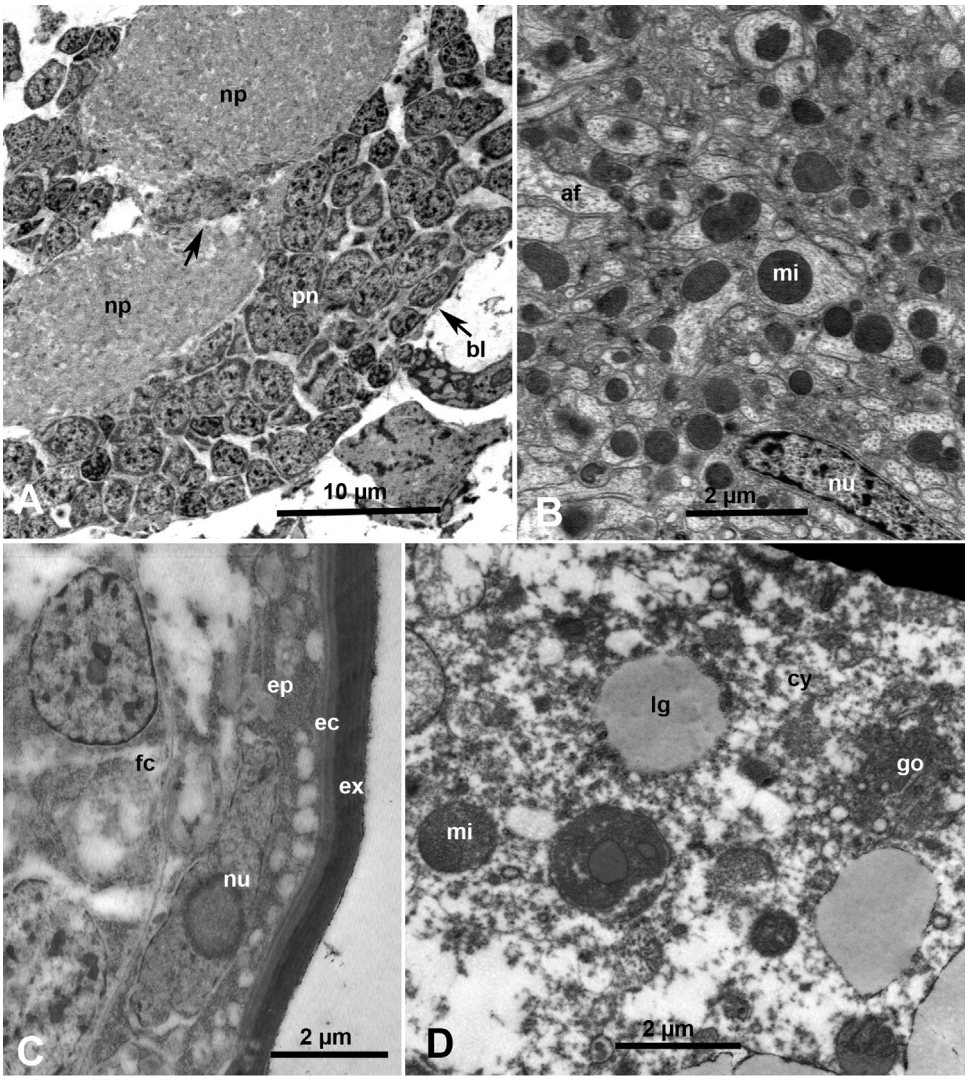

Fig. 7. Ultrastructure of neural, epidermal and fat cells in *Diaphorina citri*. (A) Sagittal section in part of the compound ganglionic mass in the thorax, showing basal lamina (bl), neural cells of the perineurium (pn), surrounding neural fibers of the neuropile (np); note constriction of the neuropile (unlabeled arrow). (B) Details of an axon showing abundant mitochondria (mi), axon filaments (af) and elongated nucleus (nu). (C) An epidermal cell (ep) with elongated nucleus (nu) and excreted layers of endocuticle (ec) and exoculticle (ex); fc, underlying fat cell. (D) Part of a large fat cell, showing lipid granules (lg), mi, Golgi organelle (go) and cytoplasm (cy).

reported [36–38]. In circulative and propagative transmission of plant pathogens, including those associated with HLB and other psyllid-borne diseases, these pathogens are inoculated into host plants by their insect vectors during salivation, and the efficacy of transmission may be affected by salivary secretions of the vector [39]. Thus, further work on the salivary secretions of ACP and other vectors, and the interaction of these secretions with circulative pathogen transmission, is still needed.

3.3. Alimentary canal, filter chamber, and Malpighian tubules

In ACP, the esophagus, which extended between the cibarium and the anterior-most part of the midgut inside the filter chamber, is composed of a single layer of flat epithelial cells lined with a thin layer of cuticular intima around the lumen (Figure 5A). The anatomy of the alimentary canal in ACP and the potato psyllid has been described by Cicero et al. [24] but without many ultrastructural details. Ultrastructure of ACP midgut cells is different between those parts inside the filter chamber (Figure 5B) and those outside it (Figure 5C). Parts of the anterior and posterior midgut inside the filter chamber are composed of flat epithelial cells, with long thin nuclei, and basal lamina that are closely apposed to one another (Figure 5B), apparently to enable the exchange of water between the anterior and posterior ends of the midgut, as reported in other Hemiptera [22,23]. The filter chamber complex is enclosed in a thin membranous wall (Figure 5B, cw). In the free part of the ACP midgut (outside the filter chamber), a single layer of large epithelial cells, with abundant mitochondria, largely vacuolated cytoplasm, and fairly large nuclei, surrounded a star-shaped lumen lined with extensive microvilli (Figures 5C and 6A). The basal plasma membrane of these epithelial cells is highly convoluted, with deep infoldings under the basal lamina. These epithelial cells are surrounded by a thin layer of muscle fibers, covered by another basal lamina (Figure 6A, bl). Epithelial cells of the Malpighian tubules were also vacuolated and lined with extensive microvilli, and some of their vacuoles/vesicles contained dark staining probably secretory material (Figure 6B).

Inside the filter chamber, the posterior part of the midgut empties its contents into the hindgut, which is a long narrow tube that starts inside the filter chamber and continues outside it extending posteriorly to end with a wider rectum that opens into the anus [24]. Ultrastructurally, the hindgut contains a single layer of epithelial cells bound by the basal lamina surrounded by a fairly thick layer of muscle fibers (Figure 6C). The epithelial cells contain large nuclei and abundant mitochondria, and are lined apically with a thin layer of cuticular intima around the lumen (Figure 6C). In ACP and at least two other studied psyllid species, the circum-anal ring, surrounding the anal opening in nymphs and adult females (but not in males), contains the openings of the subcuticular wax glands that produce waxy material covering the honeydew during its excretion [21,40,41]. Interestingly, nymphs and adult females of ACP and the melaleuca psyllid, *Boreioglycaspis melaleucae*, were recently reported to differ from males in their honeydew excretion behavior; apparently to protect the eggs and nymphs from being drowned, contaminated or immobilized by the sticky honeydew excretions at least in these studied psyllid species [40,41].

3.4. Neural, epidermal, and fat tissues

The central nervous system in most studied hempiterans is composed of the brain (supraesophageal ganglion), the subesophageal ganglion, and an amalgamation of the abdominal and thoracic ganglia; termed by various authors as the thoracic ganglion [21], compound ganglion [22,23], and probably more appropriately the CGM [11]. In both the subesophageal ganglion and the CGM, most of the neural cell bodies (perineurium) were situated in the periphery (Figure 7A) bound by the basal lamina, whereas the central core of each ganglion (neuropile) is composed of large and small nerve fibers (Figures 7A, np, and 7B) forming a complex fiber network [22,23]. The central core of the CGM in ACP seems to be constricted in some areas; possibly representing two or more masses each representing the amalgamation of the abdominal and thoracic ganglia (Figure 7A, arrow).

A single layer of epidermal narrow flat cells with small flattened nuclei, lined with the basal lamina, is found underneath the cuticle (Figure 7C). During molting/ecdysis, these cells produce the inner (endocuticle) and outer (exoculticle) layers of the cuticle in each instar during the nymphal and adult stages (Figure 7C). Under the epidermal layer, and in many areas throughout the hemocoel, fat tissue composed of fat cells with large nuclei, abundant endoplasmic reticulum, mitochondria and semi-opaque lipid droplets/vesicles, are found (Figures 7C and 7D).

3.5. Bacteriome and bacterium-like structures

The bactriome (formerly the mycetome) is a specialized organ, containing bacterial endosymbionts, found

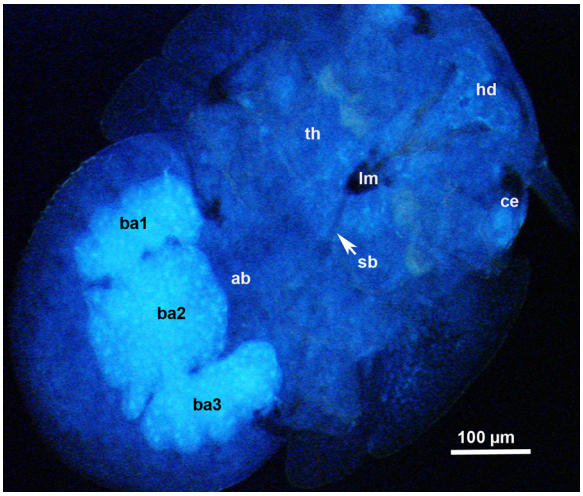

Fig. 8. Epifluorescence micrograph showing three lobes of the bacteriome (ba1, ba2, and ba3) with bright blue fluorescence, in the abdomen (ab) of a 3rd instar nymph of *Diaphorina citri*; ce, compound eye.
hd, head; lm, labium; sb, stylet bundle; th, thorax.

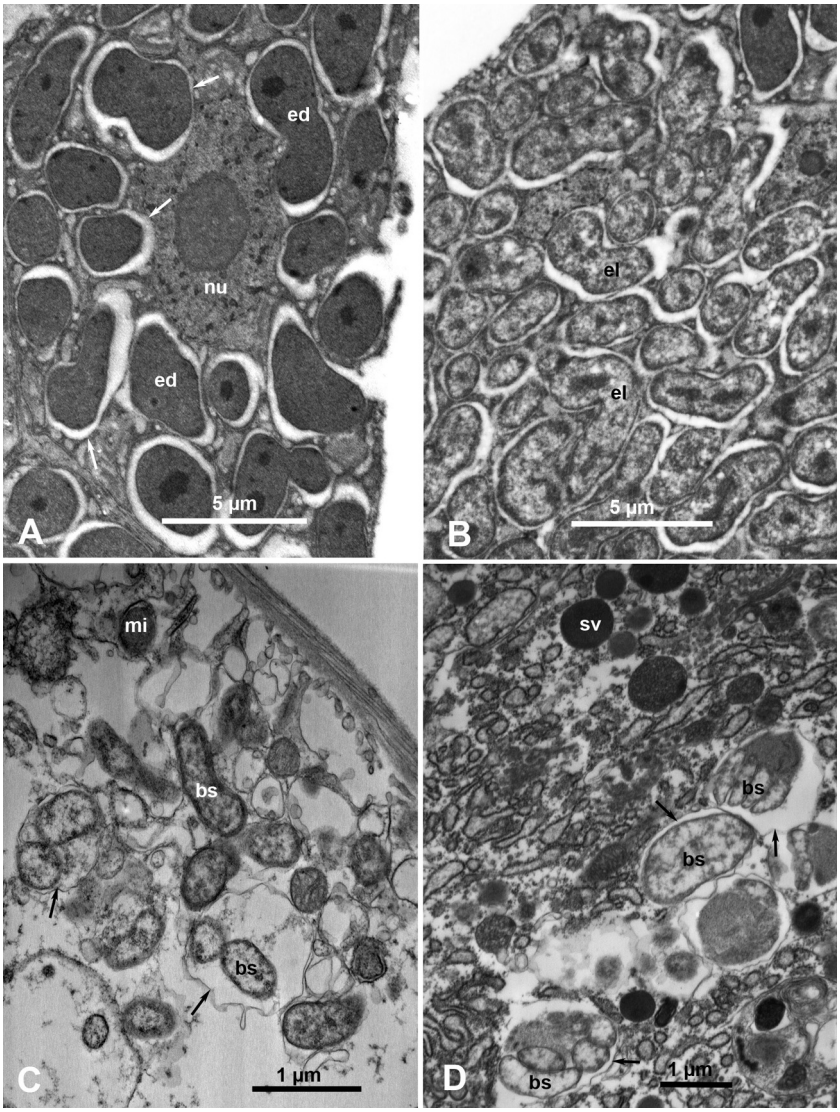

Fig. 9. Bacterium-like structures found in *Diaphorina citri* nymphs (A, B) and adults (C, D). (A) Bacteriocyte cell in the bacteriome, with a large nucleus (nu) and electron-dense bacterial cells (ed) inside membranous vesicles (arrows) in the cytoplasm. (B) Syncytial part of the bacteriome with electrolucent bacterial cells (el). (C, D) Bacterium-like structures (bs) mostly inside membranous vesicles (arrows) in the cytoplasm of a midgut epithelial cell (C) and in a salivary gland cell (D).
mi, mitochondrion; sv, secretory vesicles.

in hemipteran insects [22,23,42,43]. In psyllids, the most common bacteriome described consists of a large multinucleate syncytium, within which are uninucleate bacteriocytes. The latter contain a polymorphic bacterium, called *Candidatus* Carsonella ruddii, whereas the syncytial region of the bacteriome may also harbor a morphologically distinct (secondary) S-endosymbiont [43,44]. In fixed whole nymphs of *D. citri* (1^{st}–3^{rd} instars), the bacteriome appeared by autofluorescence as two bright blue, lateral, oblong bodies connected to a centrally located larger rectangular body in the middle of the abdomen (Figure 8, ba1–ba3). This is similar in shape and location to the bacteriome reported in the nymphs of another psyllid, *Glycaspis brimblecombei* Moore [43]. However, in psyllid adults, generally, the yellowish bacteriome becomes more branched or fragmented in the abdomen apparently by the growing reproductive organs, and some of its fragments may be found between the ovarioles [42]. Some of the bacterial endosymbionts in hemiptera are essential for the life of the insect, and thus are vertically transmitted through the ovaries/eggs to the following generations [42].

In the ACP nymphs bacteriome, two morphologically distinct, more or less rod-shaped, bacterium-like structures were found: electron-dense cells found inside the bacteriocytes (Figure 9A, ed) and electrolucent cells found in the synchytial cytoplasm (Figure 9B, el). Several bacterial microbiota (presumed to be endosymbionts), including *C.* Carsonella ruddii and *Wollbachia* spp., were detected in ACP and the potato psyllid *B. cockerelli* using molecular/PCR methods, but the ultrastructure and localization of these

endosymbionts in these insects have not been elucidated [44–46].

In addition to the above bacterial structures found inside the ACP bacteriome, other bacterium-like structures of various shapes and sizes (rod-shaped, banana-shaped, oblong, or quasispherical), ranging from 0.60 μm to 2.18 μm in length and from 0.15 μm to 0.73 μm in width, were found mostly inside membranous vesicles in the cytoplasm of midgut epithelial cells (Figure 9C, bs) and in secretory cells of the principal salivary gland (Figure 9D, bs). These bacterium-like structures were found in both qPCR-negative (presumably uninfected) ACP adults (Figures 9C and 9D) and in qPCR-positive (Las-infected) ACP adults (data not shown). It is not known whether these bacteria are plant or insect pathogens or endosymbionts that reside outside the bacteriome, for example, *Wollbachia* spp. *Rickettsia*-, and other bacterium-like structures have been reported in cells of the gut, salivary glands, and other organs of the planthopper *Peregrinus maidis* [47]. These results show that it is difficult, if not impossible, to decide which of these bacterium-like structures represent Las or other HLB-associated bacteria without immunolabeling, fluorescence *in situ* hybridization, or other reliable labeling techniques. Thus, previous reports of finding HLB-causing bacteria in cells of vector psyllids without any labeling [13–15] must be regarded as preliminary or doubtful, unless they are substantiated with further studies using some reliable labeling techniques.

In conclusion, it is hoped that this ultrastructural study of ACP organs and tissues will help future investigations on vector relations, transmission barriers, binding and receptor sites, and cellular and subcellular localization of Las, Lso or other psyllid-borne pathogens in their vector insects, especially when reliable immunolabeling techniques for such pathogens become available.

Conflicts of interest

All authors declare no conflicts of interest. This article reports the results of research only. Mention of a trademark or proprietary product is solely for the purpose of providing specific information and does not constitute a guarantee or warranty of the product by the United States Department of Agriculture and does not imply its approval to the exclusion of other products that may also be suitable. USDA is an equal opportunity provider and employer.

Acknowledgments

We thank Kathy Moulton for rearing and qPCR testing of the psyllids, and Tawheda Ammar for microtomy and ultrathin sectioning. Funds for this research were partially provided by the Florida Citrus Research and Development Foundation.

References

[1] Hodkinson ID. Life cycle variation and adaptation in jumping plant lice (Insecta: Hemiptera: Psylloidea): a global synthesis. J Nat Hist 2009;43(1-2):65–179.
[2] Gottwald TR. Current epidemiological understanding of citrus huanglongbing. Annu Rev Phytopathol 2010;48:119–39.
[3] Halbert SE, Manjunath KL. Asian citrus psyllids (Sternorrhyncha: Psyllidae) and greening disease of citrus: A literature review and assessment of risk in Florida. Florida Entomologist 2004;87:330–53.
[4] Hall DG, Richardson ML, Ammar ED, Halbert SE. Asian citrus psyllid, *Diaphorina citri* (Hemiptera: Psyllidae), vector of citrus huanglongbing disease. Entom Exp Applic 2013;146:207–23.
[5] Bové JM. Huanglongbing:A destructive, newly-emerging, century-old disease of citrus. J Plant Pathol 2006;88:7–37.
[6] Pelz-Stelinski KS, Brlansky HR, Ebert TA, Rogers ME. Transmission parameters for *Candidatus* Liberibacter asiaticus by Asian citrus psyllid. J Econ Entom 2010;103:1531–41.
[7] Inoue H, Ohnishi J, Ito T, Tomimura K, Miyata S, Iwanami T, et al. Enhanced proliferation and efficient transmission of *Candidatus* Liberibacter asiaticus by adult *Diaphorina citri* after acquisition feeding in the nymphal stage. Ann App Biol 2009;155:29–36.
[8] Sengoda VG, Buchman JL, Henn DC, Pappu HR, Munyaneza JE. *Candidatus* Liberibacter solanacearum" titer over time in *Bactericera cockerelli* (Hemiptera: Triozidae) after acquisition from infected potato and tomato Plants. J Econ Entom 2013;106:1964–72.
[9] Cooper WR, Sengoda VG, Munyaneza JE. Localization of '*Candidatus* Liberibacter solanacearum' (Rhizobiales: Rhizobiaceae) in *Bactericera cockerelli* (Hemiptera: Triozidae). Ann Entomol Soc Am 2014;107:204–10.
[10] Ammar ED, Shatters Jr RG, Hall DG. Localization of *Candidatus Liberibacter asiaticus*, associated with citrus huanglongbing disease, in its psyllid vector using fluorescence *in situ* hybridization. J Phytopathol 2011;159:726–34.
[11] Ammar ED, Shatters RG, Lynch C, Hall DG. Detection and relative titer of *Candidatus* Liberibacter asiaticus in the salivary glands and alimentary canal of *Diaphorina citri* (Hemiptera: Psyllidae) vector of citrus huanglongbing disease. Ann Entom Soc Am 2011;104:526–33.
[12] Cicero JM, Fisher TW, Brown JK. Localization of '*Candidatus* Liberibacter solanacearum' and evidence for surface appendages in the potato psyllid vector. Phytpathology 2016;106:142–54.
[13] Chen MH, Miyakawa T, Matsui C. Citrus Likubin pathogen in salivary glands of *Diaphorina citri*. Phytopathology 1973;63:194–5.
[14] Xu CF, Xia YH, Li KB, Ke C. Further study of the transmission of citrus huanglongbing by a psyllid, Diaphorina citri Kuwayama. In: Timmer LW, Garnsey SM, Navarro L, editors. Proceedings of the 10th Conference of the International Organization of Citrus Virologists, 17-21 November 1986, Valencia, Spain. International Organization of Citrus Virologists, University of California, Riverside, CA, USA; 1988, p. 243-8.
[15] Moll JN, Martin MM. Electron microscope evidence that citrus psylla (*Trioza erytreae*) is a vector of greening disease in South Africa. Phytophylactica 1973;5:41–4.
[16] Ammar ED, Hogenhout SA. Mollicutes associated with arthropods and plants. In: Kostas B, Miller T, editors. Insect symbiosis Vol. II. Boca Raton: CRC Press, Taylor & Francis Group; 2006. p. 97–118.
[17] Ammar ED, Tsai CW, Whitfield AE, Redinbaugh MG, Hogenhout SA. Cellular and molecular aspects of rhabdovirus interactions with insect and plant hosts. Annu Rev Entomol 2009;54:447–68.
[18] Li WB, Hartung JS, Levy L. Quantitative real-time PCR for detection and identification of *Candidatus* Liberibacter species associated with citrus huanglongbing. J Microbiol Methods 2006;66:104–15.
[19] Ammar ED. Ultrastructure of the salivary glands of the planthopper *Peregrinus maidis* (Homoptera, Delphacidae). Int J Insect Morphol Embryol 1986;15:417–28.
[20] Ammar ED, Hall DG. New and simple methods for studying hemipteran stylets, bacteriomes, and salivary sheaths in host plants. Ann Entomol Soc Am 2012;105:731–9.
[21] Brittain WH. The morphology and synonymy of *Psylla mali* Schmidberger. Proc Acadian Entomol Soc 1923;8:23–42.
[22] Ammar ED. Internal morphology and ultrastructure of leafhoppers and planthoppers. In: Nault LR, Rodriguez JG, editors. Leafhoppers and planthoppers. New York: Wiley; 1985. p. 121–62.
[23] Chapman RF. The insects: structure and function. 5th edition Cambridge: Cambridge Univ Press; 2013.
[24] Cicero JM, Brown JK, Roberts PD, Stansly PA. The digestive system of *Diaphorina citri* and *Bactericera cockerelli* (Hemiptera: Psyllidae). Ann Entomol Soc Am 2009;102:650–65.
[25] Cicero JM, Stansly PA, Brown JK. Functional anatomy of the oral region of the potato psyllid (Hemiptera: Psylloidea: Triozidae). Ann Entomol Soc Am 2015;108:743–61.
[26] Marchini D, Bene GD, Viscuso R, Dallai R. Sperm Storage by spermatodoses in the spermatheca of Trioza alacris (Flor, 1861) Hemiptera,

Psylloidea, Triozidae: A structural and ultrastructural study. J Morphol 2012;273:195–210, 2012.
[27] Dossi FCA, Cônsoli FL. Gross morphology and ultrastructure of the female reproductive system of *Diaphorina citri* (Hemiptera: Liviidae). Zoologia 2014;31:162–9.
[28] Wayadande AC, Baker GR, Fletcher J. Comparative ultrastructure of the salivary glands of two phytopathogen vectors, the beet leafhopper, *Circulifer tenellus* (Baker), and the corn leafhopper, *Dalbulus maidis* Delong and Wolcott (Homoptera: Cicadellidae). Int J Insect Morphol Embryol 1997;26:113–20.
[29] Sogawa K. Studies on the salivary glands of rice plant leafhoppers. I. Morphology and histology. Jpn J Appl Entomol Zool 1965;9:275–90, 1965.
[30] Ghanim M, Rosell RC, Campbell LR, Czosnek H, Brown JK, Ullman DE. Digestive, salivary, and reproductive organs of *Bemisia tabaci* (Gennadius) (Hemiptera: Aleyrodidae) B Type. J Morph 2001;248:22–40.
[31] Reis MM, Meirelles RMS, Soares MJ. Fine structure of the salivary glands of *Triatoma infestans* (Hemiptera: Reduviidae). Tissue Cell 2003;35:393–400.
[32] Smith DS. Insect cells: their structure and function. Edinburgh: Oliver & Boyd; 1968.
[33] Ponsen MB. Anatomy of an aphid vector: *Myzus persicae*. In: Harris KF, Maramorosch K, editors. Aphids as virus vectors. New York: Academic Press; 1977. p. 63–82.
[34] Raine J, Forbes AR. The salivary syringe of the leafhopper *Macrosteles fascifrons* (Homoptera: Cicadellidae) and the occurrence of Mycoplasma-like organisms in its ducts. Can Entomol 1971;103:110–6.
[35] Will T, Steckbauer K, Hardt M, van Bel AJE. Aphid gel saliva: sheath structure, protein composition and secretory dependence on stylet-tip milieu. PLoS ONE 2012;7:e46903.
[36] Miles PW. Aphid saliva. Biol Rev 1999;74:41–85.
[37] Cooper WR, Dillwith JW, Puterka GJ. Comparisons of salivary proteins from five aphid (Hemiptera: Aphididae) species. Environ Entomol 2011;40:151–6.
[38] Huang HJ, Liu CW, Cai YF, Zhang MZ, Bao YY, Zhang CX. A salivary sheath protein essential for the interaction of the brown planthopper with rice plants. Insect Biochem and Molec Biol 2015;66:77–87.
[39] Ammar LD. Propagative transmission of plant and animal viruses by insects: factors affecting vector specificity and competence. Adv Dis Vector Res 1994;10:289–332.
[40] Ammar L-D, Alessandro R, Shatters Jr RG, Hall DG. Behavioral, ultrastructural and chemical studies on the honeydew and waxy secretions by nymphs and adults of the Asian citrus psyllid *Diaphorina citri* (Hemiptera: Psyllidae). PLoS ONE 2013;8:e64938.
[41] Ammar E-D, Hentz M, Hall DG, Shatters RG. Ultrastructure of wax-producing structures on the integument of the melaleuca psyllid *Boreioglycaspis melaleucae* (Hemiptera: Psyllidae), with honeydew excretion behavior in males and females. PLoS ONE 2015;10:e0121354.
[42] Buchner P. Symbiosis in animals which suck plant juices. In: Endosymbiosis of animals with plant microorganisms. New York: Interscience; 1965. p. 210–432.
[43] Baumann P. Biology of bacteriocyte-associated endosymbionts of plant sap-sucking insects. Annu Rev Microbiol 2005;59:155–89.
[44] Meyer JM, Hoy MA. Molecular survey of endosymbionts in Florida populations of Diaphorina citri (Hemiptera: Psyllidae) and its parasitoids Tamarixia radiata (Hymenoptera: Eulophidae) and Diaphorencyrtus aligarhensis (Hymenoptera: Encyrtidae). Florida Entomologist 2008;91:294–304.
[45] Nachappa P, Levy J, Pierson E, Tamborindeguy C. Diversity of endosymbionts of the potato psyllid, *Bactericera cockerelli* (Hemiptera: Triozidae), vector of zebra chip disease of potato. Current Microbiol 2011;62:1510–20.
[46] Saha S, Hunter WB, Reese J, Morgan JK, Marutani-Hert M, et al. Survey of endosymbionts in the *Diaphorina citri* metagenome and assembly of a Wollbachia wDi Draft Genome. PLoS ONE 2012;7:e50067.
[47] Ammar LD, Nault LR, Styer WE, Saif M. *Staphylococcus*, Paramyxovirus-like, *Rickettsia*-like and other structures in *Peregrinus maidis* (Homoptera, Delphacidae). J Invert Pathol 1987;49:209–17.